

# Acoustic Sensor Array Extracts Physiology During Movement

Michael V. Scanlon, US Army Research Laboratory, Adelphi, MD 20783-1197 [mscanlon@arl.army.mil](mailto:mscanlon@arl.army.mil)

## ABSTRACT

An acoustic sensor attached to a person's neck can extract heart and breath sounds, as well as voice and other physiology related to their health and performance. Soldiers, firefighters, law enforcement, and rescue personnel, as well as people at home or in health care facilities, can benefit from being remotely monitored. ARL's acoustic sensor, when worn around a person's neck, picks up the carotid artery and breath sounds very well by matching the sensor's acoustic impedance to that of the body via a gel pad, while airborne noise is minimized by an impedance mismatch. Although the physiological sounds have high SNR, the acoustic sensor also responds to motion-induced artifacts that obscure the meaningful physiology. To exacerbate signal extraction, these interfering signals are usually covariant with the heart sounds, in that as a person walks faster the heart tends to beat faster, and motion noises tend to contain low frequency components similar to the heart sounds. A noise-canceling configuration developed by ARL uses two acoustic sensors on the front sides of the neck as physiology (plus noise) sensors, and two additional acoustic sensors on the back sides of the neck as noise references. Breath and heart sounds, which occur with near symmetry and simultaneity at the two front sensors, will correlate well. The motion noise present on all four sensors will be used to cancel the noise on the two physiology sensors. This report will compare heart rate variability derived from both the acoustic array and from ECG data taken simultaneously on a treadmill test. Acoustically derived breath rate and volume approximations will be introduced as well. A miniature 3-axis accelerometer on the same neckband provides additional noise references to validate footfall and motion activity.

Keywords: Acoustic, sensor, physiology, monitor, IBI, heart, breath, blood pressure, health, performance

## 1. INTRODUCTION

The ability to continuously monitor the health and performance of soldiers and squads can provide exceptional improvements to survivability, mobility, and lethality. Body worn physiological sensors can be used for operational medicine, combat casualty care, training, simulation, performance and readiness assessment. The Army Research Laboratory (ARL) has developed acoustic sensor and signal processing technology to significantly enhance situational awareness relating to soldier health, performance, and how the soldier is interacting with the mission at hand. ARL's Acoustic Physiological Monitoring program's objective is to investigate acoustic sensor technology for monitoring human health and performance to potentially support the Warfighter Physiological Status Monitor (WPSM), Land Warrior (LW), Warrior Medic, Military Operations in Urban Terrain Advanced Concept Technology Demonstration (MOUT ACTD), Future Combat Systems (FCS), and other military and civilian programs relating to health monitoring of firefighters, law enforcement, recovering patients, and personal monitoring. By using an acoustic sensor in contact with the soldier's body, heart, lung, and other diverse physiology can be detected with significant signal to noise ratio over ambient sounds. The sensor consists of a fluid or gel contained within a small, conformable, rubber bladder or pad that also includes a hydrophone. By knowing the instantaneous status of a person's physiology, and knowledge of previous trends, leaders or medics can make informed manpower decisions that can improve the probability of mission success. Commanders can choose the most rested squads. Medics can perform remote triage to prioritize treatments or determine if the medic should risk his own life to rescue a soldier lying still in the middle of a landmine field or in the sights of a sniper.

The ARL developed sensor technology monitors a soldier's voice very well when contacting the throat region. It is low cost and comfortable to wear for extended periods. ARL further developed (with support from the United States Military Academy), a Hidden-Markov Model (HMM) phoneme-level speech system optimized for the physiological sensor package. Data collected shows tremendous potential for the physiological sensor's use in automatic speech recognition under quiet and very high noise conditions. [Bass, et. al.] In tomorrow's digitized battlefield, every soldier needs a communication sensor, and with the increased use of soldier worn computers and automatic speech recognition for computer controls, the physiological sensor can be used for both voice and physiology with only minor software additions. Fewer sensors means less weight.

## 2. BACKGROUND

The excellent acoustic coupling that exists between a human body, which is mostly water, and a fluid-filled sensor pad enables collection of high signal-to-noise ratio heartbeat and breath signatures. This gel-filled pad acts as a fluid extension of the body to form an acoustical conduit to a sensitive hydrophone, within the pad, that detects body sounds. Details of the sensor are shown below in Figure 1 and Figure 2.

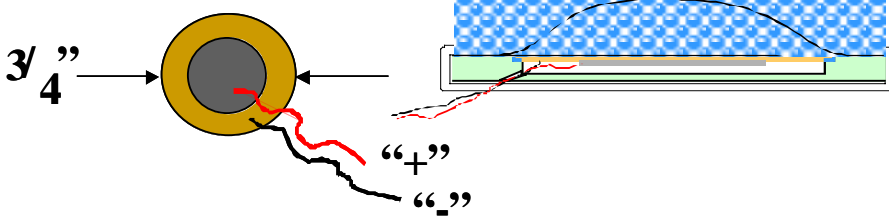


Figure 1: Piezo and assembly cross-section



Figure 2: Gel-coupled sensor

Effective attenuation of ambient background noise results from the poor coupling between the airborne noise and the fluid-filled pad. The electrical output of this transducer can be filtered, amplified, analyzed, and transmitted, depending on the specific application. Traditional diagnostic methods such as listening to the audio and looking at the voltage vs. time waveform can be augmented by joint time-frequency domain Fourier analysis techniques or wavelet based techniques.

Numerous configurations of the sensor have been fabricated and tested [Scanlon]. Torso sized arrays can be built into stretchers or operating tables. Figures 3 and 4 are wrist and neck attachment mechanisms. Sensors in helmet headbands and chest straps have been configured. Figure 5 shows the sensor signal's output directly connected to the auxiliary microphone jack of a standard palmtop computer, using wireless LAN cards to communicate with a remote laptop. By using TCP/IP protocol, the data from this sensor could be monitored by any doctor, family member, or commander via the world wide web.



Fig. 3: wrist sensor



Fig. 4: neck strap sensor



Fig.5: palmtop with RF telemetry

## 3. DATA

The quality of the acoustic data collected with the sensors is exceptional. Experimental data shown below was collected with a 12-bit PCMCIA data acquisition card in the palmtop computer shown above. The data shown in figure 6 is from an acoustic sensor on the wrist, one on the neck, and a Polar Heart Rate Monitor strapped to the chest (a bipolar electrode based commercial monitor).

As depicted in figure 6, there is a time difference of arrival associated with the electrical signals controlling the heart (as sensed by the Polar device), and the pulse pressure waves propagating to the neck and wrist. The difference shown in figure 6 is 0.064- to 0.066-s. This time difference changes with respect to blood pressure, and is directly calibratable to the systolic blood pressure [Dauzat]. Data presented later in this paper will show that the pulse transit time varies with changes in the blood pressure.

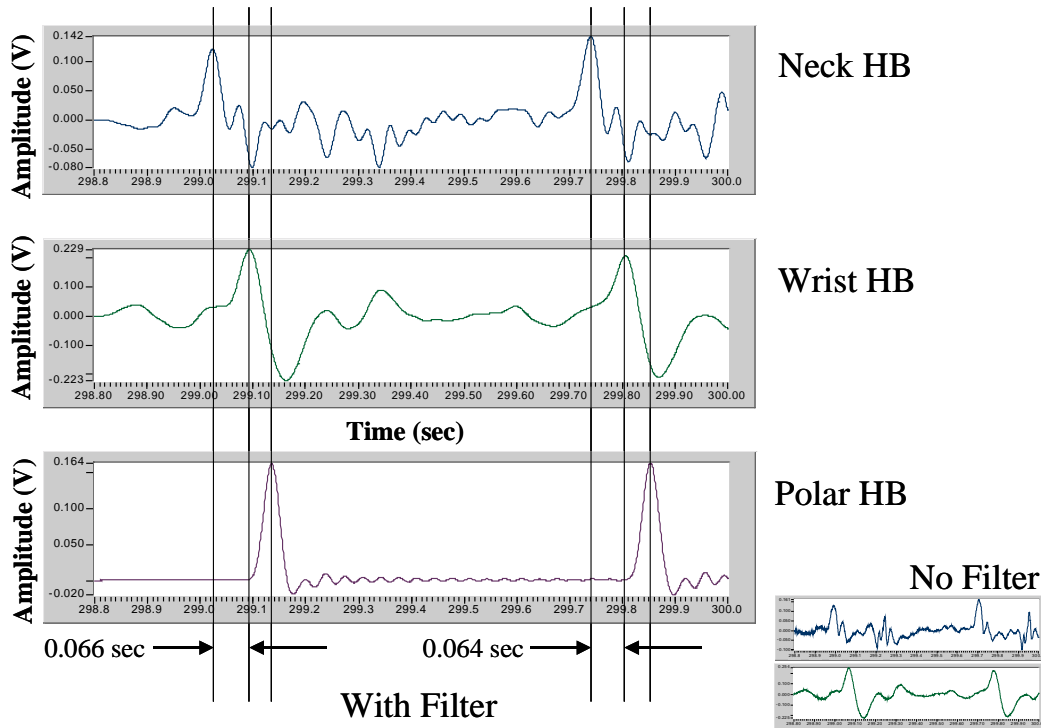


Figure 6: Sample filtered waveform from neck, wrist, and Polar monitors

Figure 7 shows the graphical definition of the 1<sup>st</sup>- to 2<sup>nd</sup>-heartsound and the inner-beat-interval (IBI), which is the time difference from one 1<sup>st</sup>-heartsound to the next 1<sup>st</sup>-heartsound. Tracking this instantaneous IBI is very important, in that it fluctuates in a known manner relative to the body's internal regulation of blood pressure, core temperature, breathing, and mental activity [Mulder].

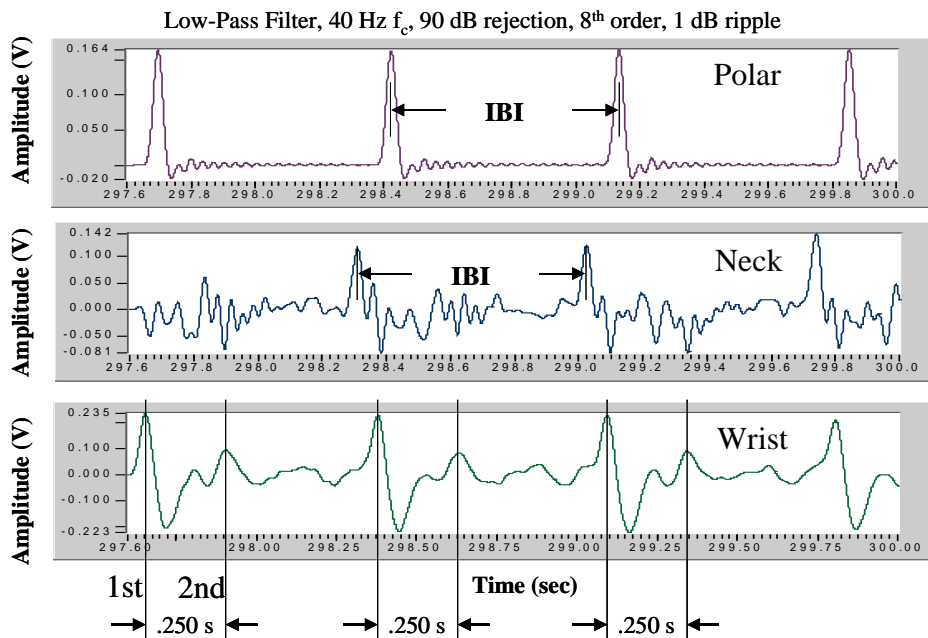


Figure 7: Inner-beat-interval and 1<sup>st</sup>- to 2<sup>nd</sup>-heartsound depiction

Algorithms process the Polar data to derive heart rate variability (HRV) to be used for truth data when assessing acoustic algorithm performance. The Polar IBI and HRV are shown in figure 8. The IBI time, in seconds, divided into 60 seconds per

minute will give the heart rate in beats per minute. An IBI of 1 second gives 60 beats per minute (BPM), whereas an IBI of 0.5 seconds gives 120 BPM.

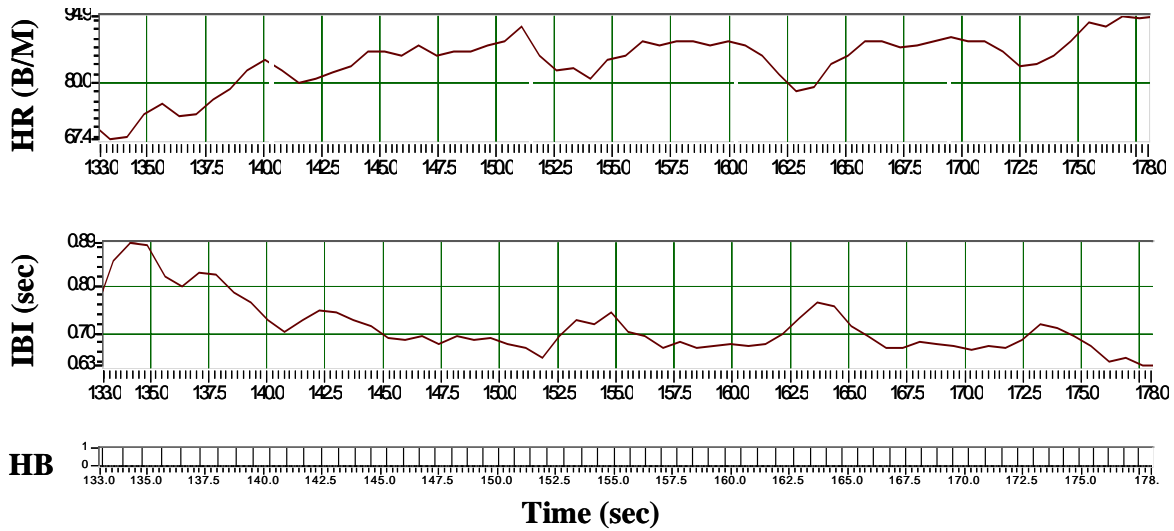


Figure 8: Heart rate, Inner-Beat-Interval, and pulse indicators from the Polar data

The sounds measured at the throat also contain excellent breath data, as shown in the acoustic data in figure 9. A high-pass filter of 400 Hz shows the structure of inhale, exhale, pause, and repeat. The envelope of the data clearly shows duration, patterns, and amplitude differences. The root-mean-squared (RMS) values of this data approximates the volume of the breaths [Kramn]. Except for asthmatic patients (most soldiers are not), this RMS data can indicate breath rates and volumes, and may be useful for calculating expended energy or breathing history.

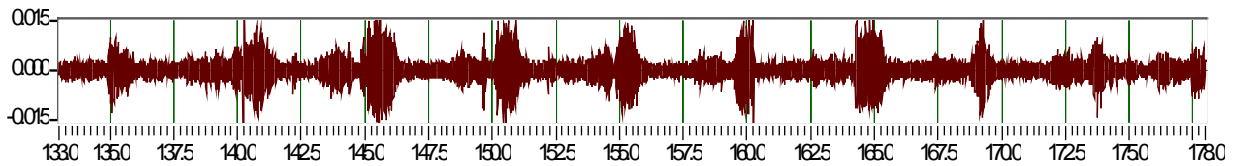


Figure 9: High-passed acoustics from throat shows breath cycle, amplitudes, and rate

#### 4. RESULTS

An experiment was conducted to demonstrate cross- and auto-correlation methods to derive IBI and HRV, and show the ability to detect the pulse wave velocity changes between the wrist and neck associated with blood pressure differences. One acoustic sensor was located at the subject’s neck, another similar acoustic sensor was located on the subjects left wrist, and the Polar monitor was strapped on the subject’s chest. Polar heart rate data was used in an auto-correlation analysis shown in figure 10 to show that using a 2048-point correlation window with a shift window of 0.4 seconds gives excellent IBI results. All data were sampled at 1500 Hz with anti-aliasing filters set at 500 Hz. A 2048-point correlation window ensured that at least two heartbeats were present for each shifted auto-correlation. The auto-correlation essentially slides a window of data over itself in a point-by-point fashion, multiplying the entire data set by it’s shifted self, and summing the result. Maximum correlation occurs when the waveforms are perfectly shifted to overlap, in that misaligned waveforms may have positive and negative components who’s product will be negative and subtract from the total. Conversely, aligned waveforms will have strong negative component correlation who’s product will be positively summed, and the positive components will have strong positive correlation that will contribute positively to the sum as well.

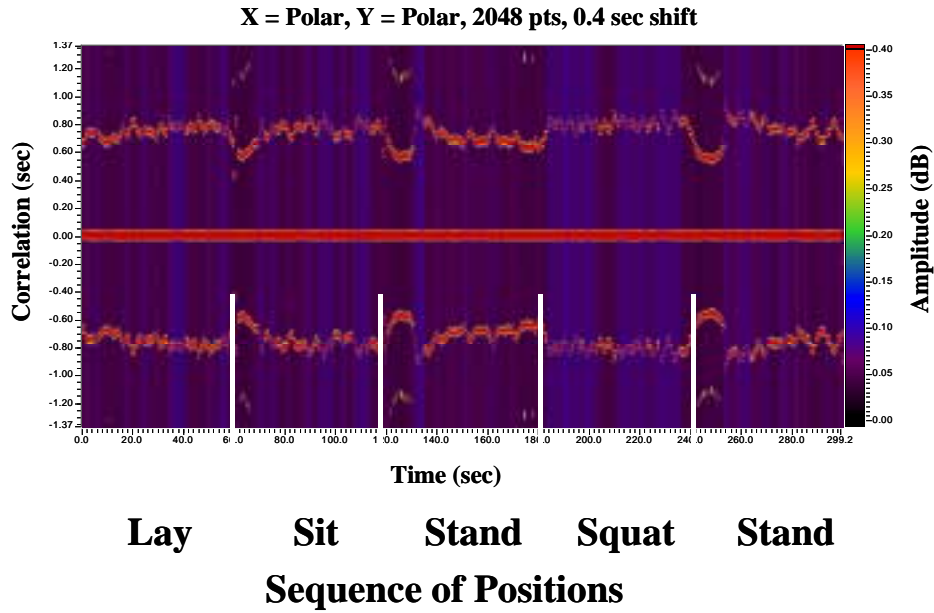


Figure 10: Auto-correlation of Polar heart monitor data showing IBI results

Five minutes of data were taken as the subject cycled through five different positions: lie, sit, stand, squat, and stand. It is common for doctors to take their patient's blood pressures and listen to heart sounds during these stances to give data under varying stress conditions without modifying heart-rate significantly. The IBI data in figure 10 shows that going from the lying to sitting position, from the sitting to standing positions, and from the squatting to standing position requires significant effort that decreases the IBI (increases the heartrate), but going from the standing to the squatting position does not result in a dramatic change in IBI since the maneuver requires minimal energy (thanks to gravity helping the subject lower to the squat position). The auto-correlation processing was applied to the acoustic data taken from the neck (figure 11) and on the acoustic data taken from the wrist (figure 12).

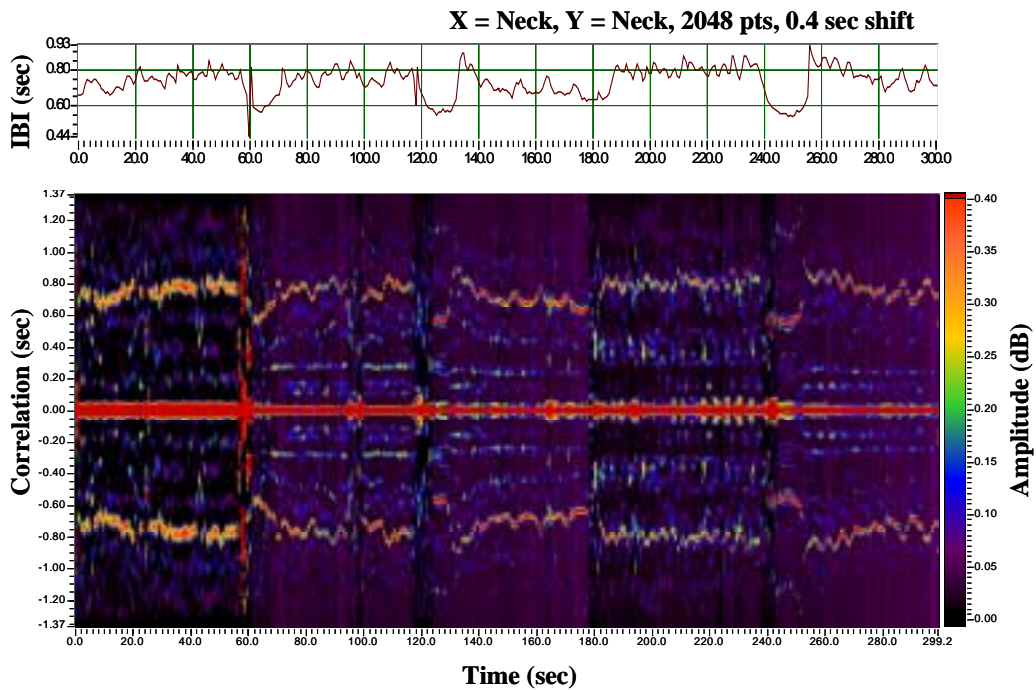


Figure 11: Auto-correlation of acoustic neck data shows IBI's match Polar truth IBI's

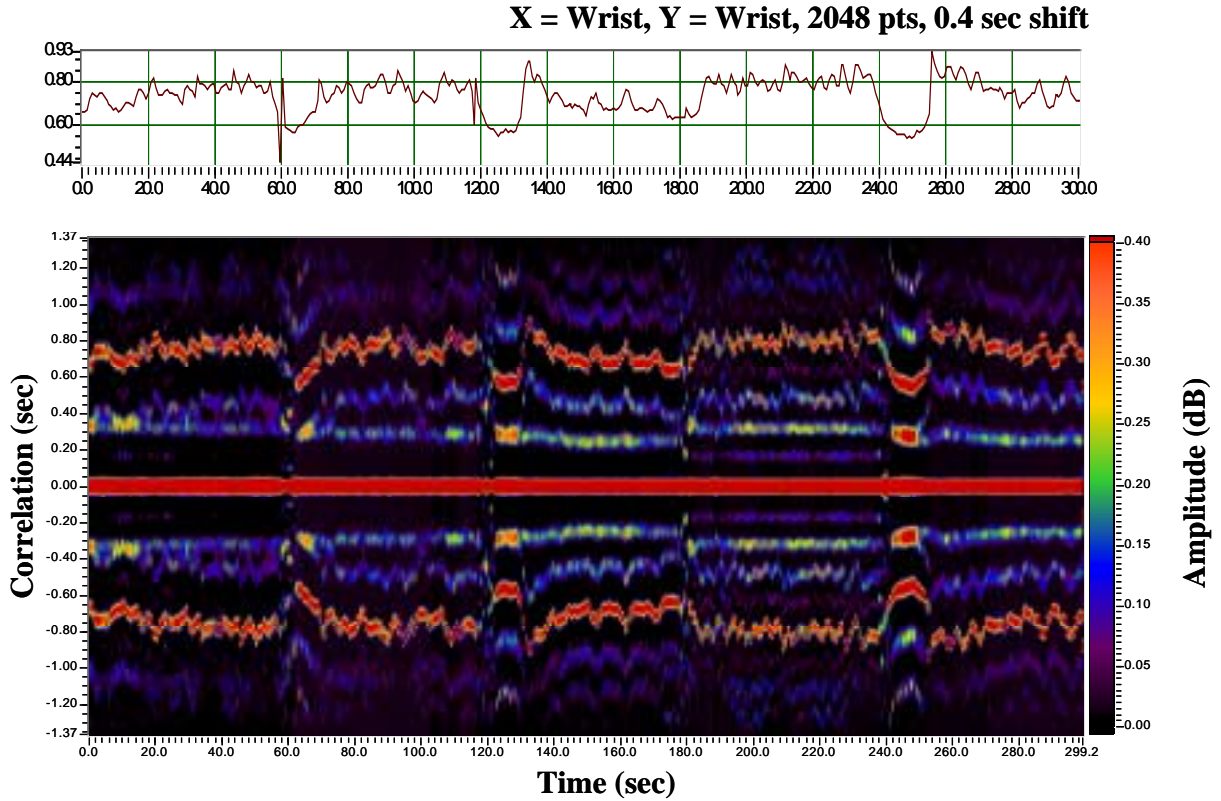


Figure 12: Auto-correlation of acoustic wrist data shows IBI's match Polar truth IBI's

Note that in figure 11, and particularly in figure 12, there are strong correlation values in the 0.3 to 0.4 region corresponding to the 1<sup>st</sup>- to 2<sup>nd</sup>-heartsound separation intervals. This is a fortunate artifact of the auto-correlation process, in that there is significant alignment of waveforms when the 1<sup>st</sup>-heartsounds align with the shifted 2<sup>nd</sup>-heartsounds, giving a strong correlation that indicates the time between events.

Combining the auto-correlation results from the wrist and the neck data will enhance the IBI detection due to the simultaneous nature of pulse events and the randomness of motion induced noise events. The interfering noise signatures and timing are very dissimilar when sensed at the wrist and neck locations. Figure 13 shows the additive combination of the individual auto-correlations from the wrist and from the neck. The IBI data SNR is clearly improved and very accurately matches the Polar heart rate truth data, as seen in the zoomed-in view of figure 14. Note that the harmonic nature of the IBI curves can be used to enhance the fundamental and further eliminate non-harmonically related motion artifacts. The 1<sup>st</sup>-to-2<sup>nd</sup> heartsound separation time is also present in figure 13.

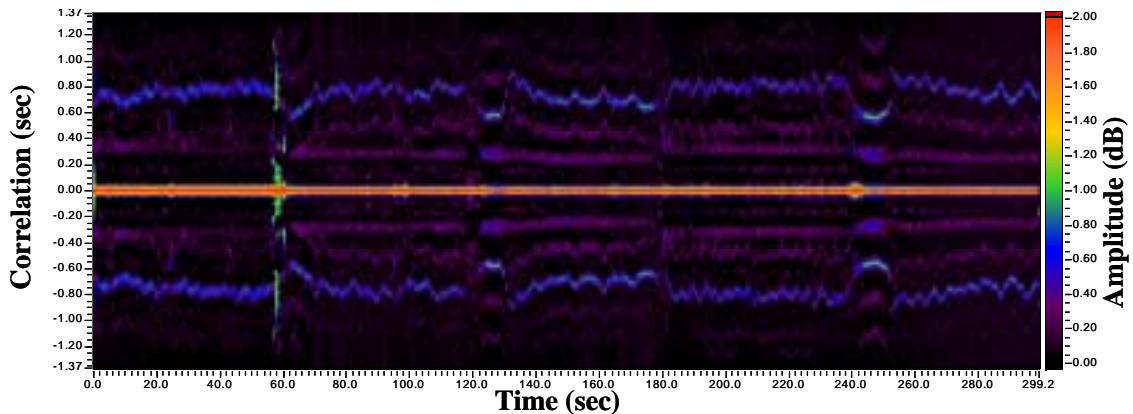


Figure 13: Sum of individual auto-correlations from wrist and neck acoustic data

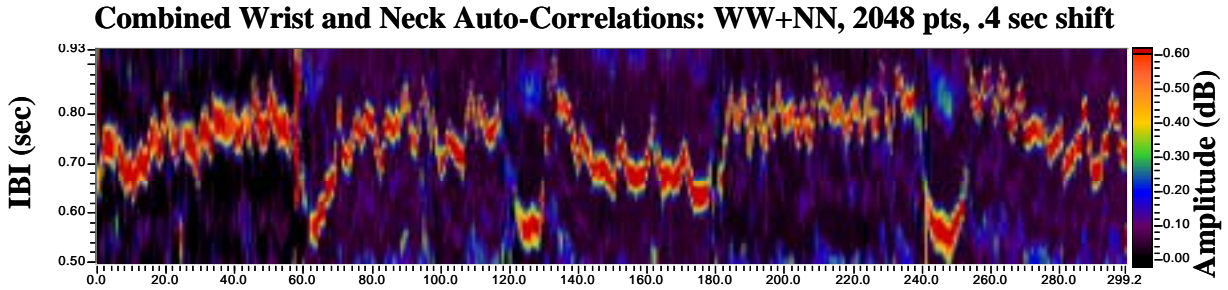


Figure 14: zoom view of IBI from combined wrist and neck auto-correlations

Figure 15 shows the cross-correlation between the neck and wrist acoustic sensors. This shows the covariant nature of the heart pulses detectable at both locations. The 1<sup>st</sup>-to-2<sup>nd</sup> heartsound separation time is also seen. As the pulsations in the neck change rate (variable IBI's), the pulses detectable at the wrist vary in sync with the neck pulse variations after a short propagation delay. The actual pulse wave delay is related to the wave propagation speed within the arteries, and is directly related to the systolic blood pressure [ref]. This result is highlighted in figure 16, which highlights the short correlation region of figure 15.

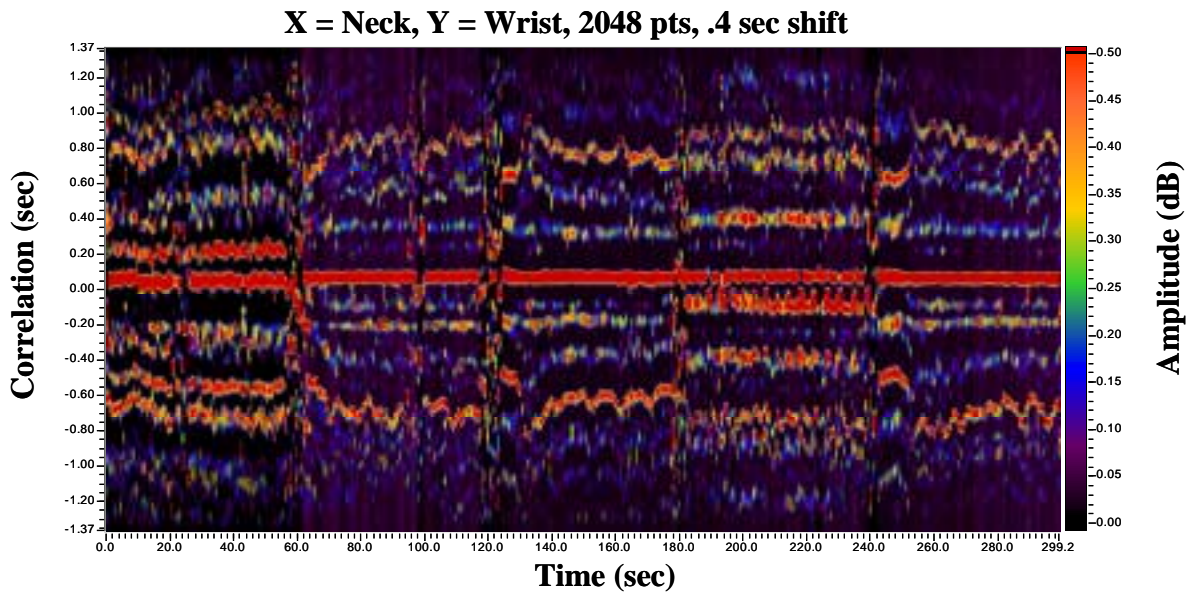


Figure 15: Cross-correlation between neck and wrist acoustic sensor data

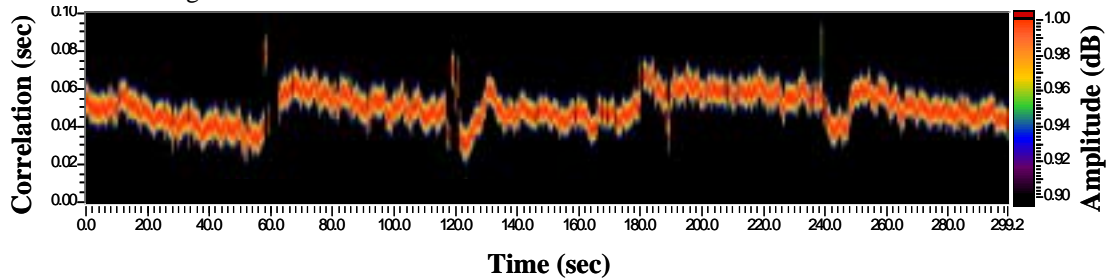


Figure 16 : Cross-correlation between neck and wrist showing blood pressure

The pulse wave transit times in figure 16 are on the order of 0.040- to 0.070-s and are reasonable delays based on crude approximations of path length and arterial pulse wave velocity (PWV) of a healthy person. The approximate path length from the subject's aorta to the wrist is 28-inches, the path length from the aorta to the neck is 10-inches, giving a differential path length of 18-inches, which at 6.6 m/s PWV, gives a 0.070 second delay. Figure 17 shows the combined auto-correlations of the individual wrist and neck acoustic data added to the cross-correlation between the wrist and neck acoustic data (add figures 13 and 15). Figure 13's contribution enhances the IBI through two diverse locations, and figure 15's contribution highlights the time shift between the neck and wrist pulse alignment. The details in the upper part of figure 17

show the sum of the correlations taken at the 137.6-second point in the entire data set. The twin-peaks circled in the graphic demonstrate the  $\sim 0.075$ -second pulse wave velocity shift between the neck and wrist.

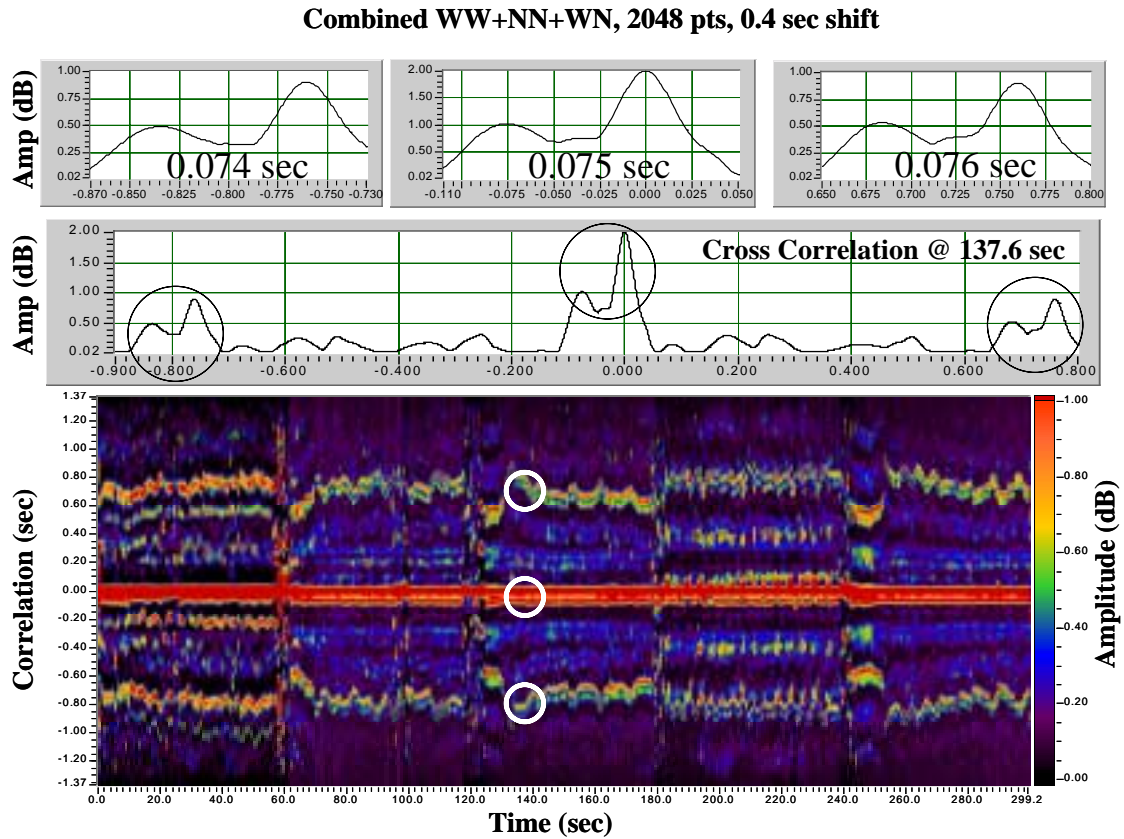


Figure 17: Sum of the wrist & neck auto-correlations with the cross-correlation between neck and wrist.

There is always an interest in sensor fusion and an inherent benefit to having redundant measures of physiology based on diverse sensing phenomena. Throughout this report the Polar heart rate monitor has been used as truth data, but the ECG sensor system is an excellent complement to the acoustic sensors. The Polar heart rate monitor is susceptible to electromagnetic interference, whereas the acoustic sensor is susceptible to motion artifacts. By having diversity in measured phenomena, there is a stronger reliability that correct physiological assessment can be ensured. Figure 18 shows the cross-correlation between the neck and Polar sensors, and Figure 19 is a zoomed view of the short correlation region of figure 18. Figure 18 shows the PWV between the electrical signal at the heartbeat onset and the resulting acoustic pulse detected at the neck.

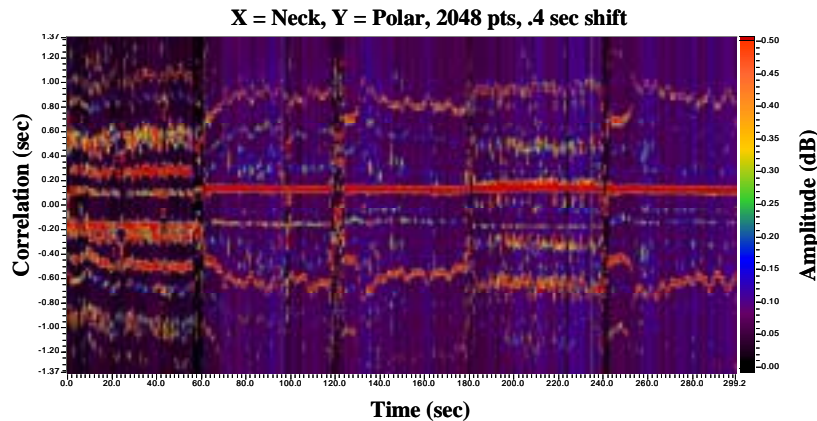


Figure 18: Cross-correlation between acoustic neck sensor and Polar ECG

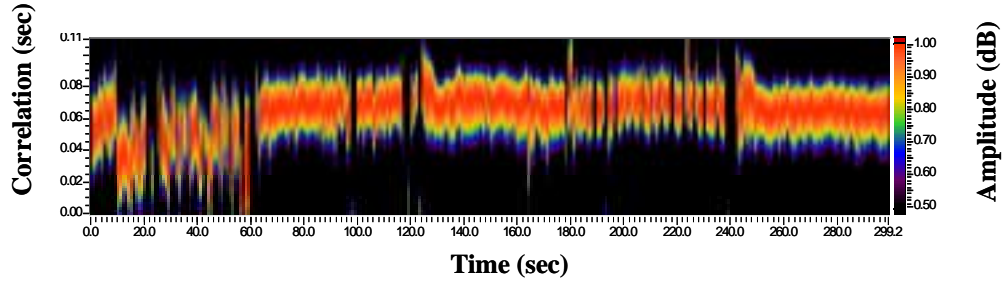


Figure 19: Cross correlation between neck and Polar, showing pulse transit time

Similarly, figures 20 and 21 show the cross-correlation between the Polar ECG and wrist acoustic sensor data. The correlation time shift in figure 21 is larger than that seen in figure 19, as expected due to the longer pulse travel length to the wrist.

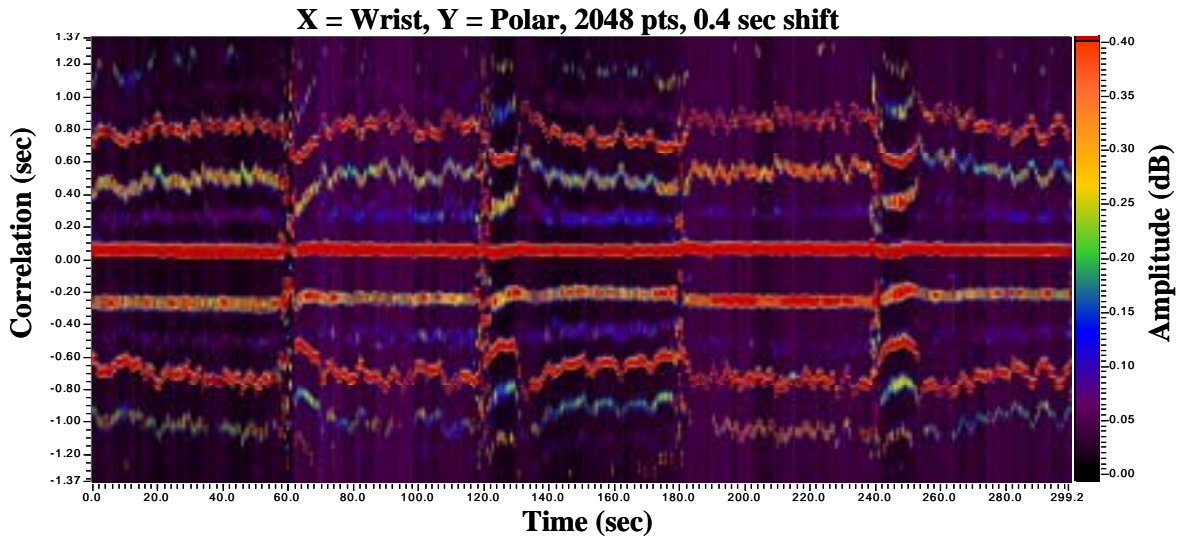


Figure 20: Cross-correlation between wrist acoustic sensor and Polar ECG

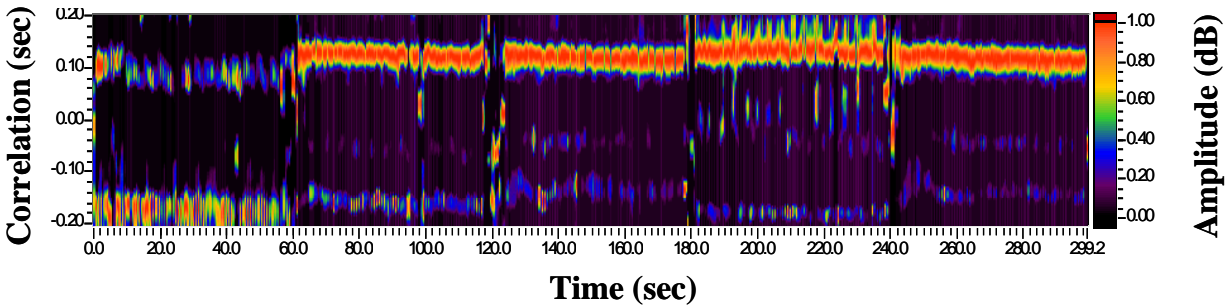


Figure 21: Cross-correlation between wrist acoustic sensor and Polar ECG

Another sensor configuration was created as a noise-canceling array to enhance the physiological signals by knowing what the noise of motion was via reference sensors. Figure 22 and figure 23 show the data collection hardware, the neck-strap sensor array, and the Polar heart rate monitor. The noise-canceling configuration has four acoustic sensors and a three-axis accelerometer. The two center acoustic sensors are positioned on the front left and right of the throat to detect physiology and noise. Since the heart, breath, and voice at these two locations are symmetrical, data from the two sensors can be added in either the time domain or after processing to enhance physiology. Noise on these two sensors does not necessarily have similar spectrum, phase, or amplitude. The two outer acoustic sensors are positioned toward the back left and right of the neck as noise references, and the accelerometer is positioned on the spine for inertial movement sensing and body acceleration forces.



Figure 22: NC array with pack



Figure 23: NC array with Polar

A quick stair climbing experiment was devised to acquire 8-channel data with a PCMCIA data acquisition card in a palmtop computer at 12-bits with a 1500 Hz sample rate with 500 Hz anti-aliasing filters. The experimental sequence went from sitting, walk to stairs, pause, climb up, turn around and climb down eight stairs, turn around at base, pause, then repeat the stair climbing cycle with pauses between each cycle. Figure 24 clearly shows the effectiveness of the acoustic sensor for detecting motion artifacts. The climbing and pause cycles are clearly visible, and footfall counts are apparent when the data is more closely viewed. Although the acoustic motion artifact data has not been compared to the Actigraph, it appears that the acoustic data may duplicate the accelerometer based wrist sensor's ability to measure patterns of sleep and movement. The Actigraph is used commercially to monitor sleep deprivation (which is very common in soldiers) and relate the data to energy expenditure.

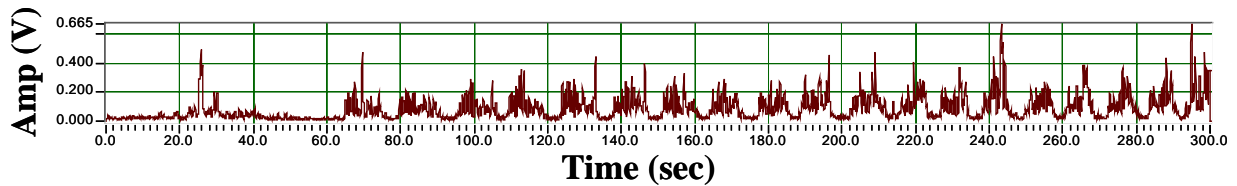


Figure 24: Acoustic representation of activity during stair climbing cycles experiment

The Polar monitor data is processed to show the IBI throughout the experiment, and are depicted in figure 25 (peak-picking algorithm) and figure 26 (auto-correlation approach). The decreasing IBI trend equates to a gradual increase in heart rate over the course of the 19 climbing cycles shown in figure 24.

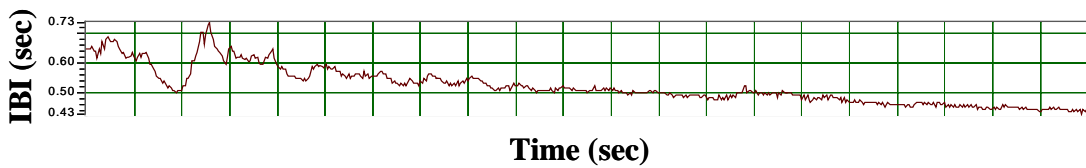


Figure 25: Polar derived inner-beat-intervals from stair climbing experiment

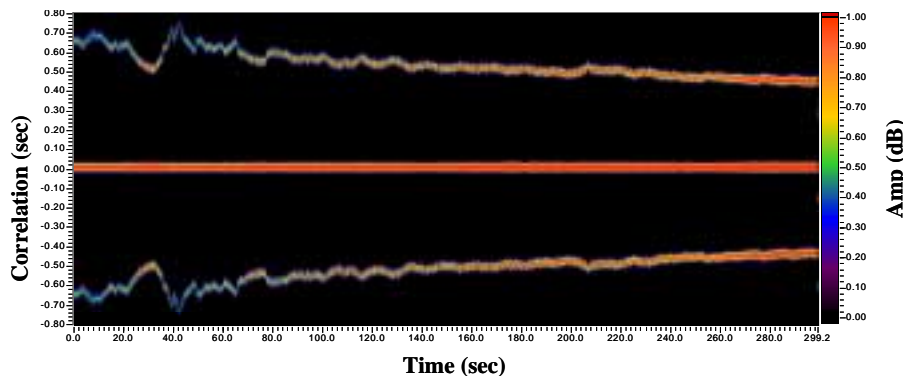


Figure 26: Auto-correlation of Polar heart rate monitor showing IBI truth data

The cross-correlation analysis between the front two acoustic “physiology” sensors is shown in figure 27, and the IBI pattern is visible. The footfalls from the stair climbing are present and sometimes mask the IBI detection. Notice that as the IBI falls, so does the impact time separation from each step. This demonstrates the common problem that as one walks faster, the heart beats faster; making it difficult to apply only temporal processing techniques, and requiring application of combined time-frequency methods. Additionally, the spectral content of body sounds resulting from footfall impacts tends to appear in the same spectral region as the heart sounds. This further confounds the spectral separation of heartbeats and footfall events. The same cross-correlation analysis between the two rear acoustic “noise reference” sensors is shown in figure 28, showing that the footfall effects are even more predominant.

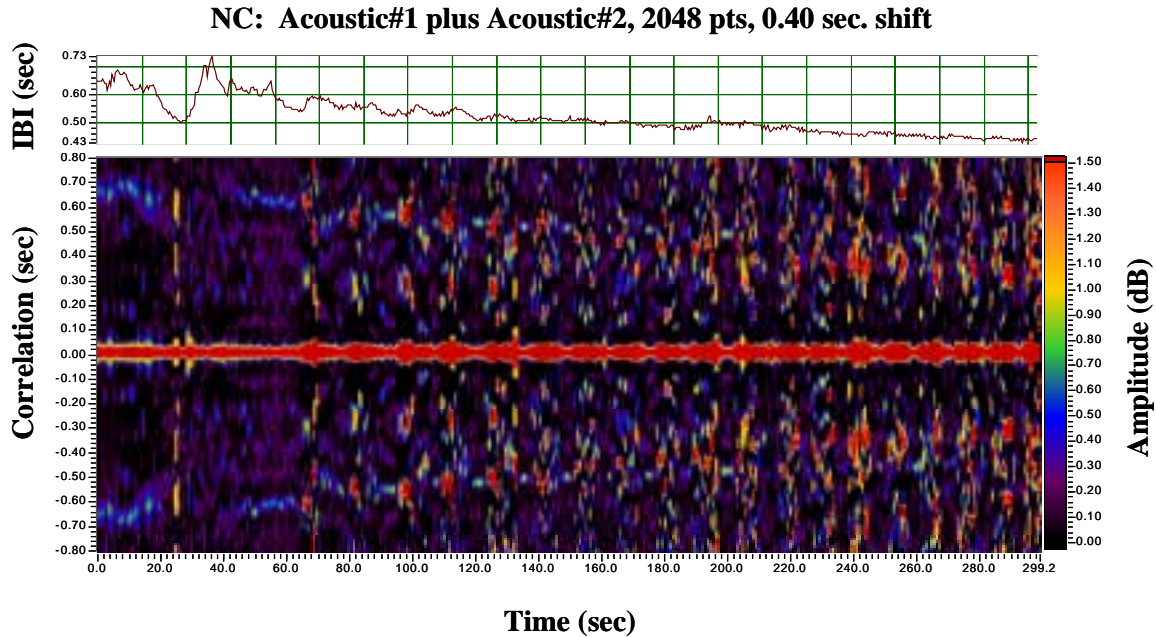


Figure 27: Cross-correlation between two frontal acoustic “physiology” sensors

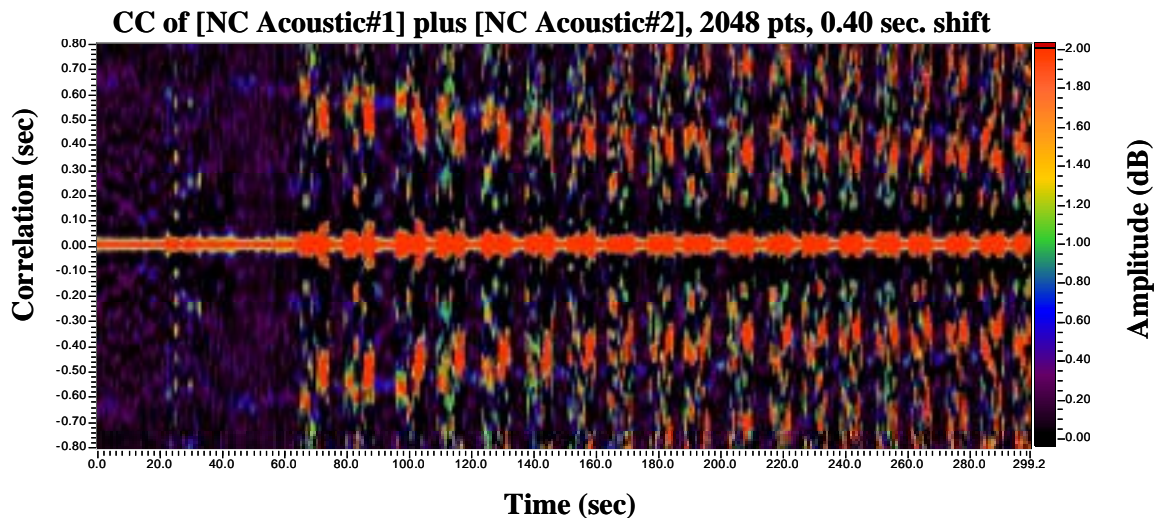


Figure 28: Cross-correlation between two rear acoustic “noise reference” sensors

It can be seen that the “noise reference” data shown in figure 28 also contains IBI (heartbeat) information. This is a result of not completely isolating the reference sensors from the heart sounds on the neck (IBI trace faintly seen). By having signal and noise on the “reference noise” it is more difficult to remove the noise without also removing the physiology. The experiment will be repeated with more effective isolation of the physiology from the noise (primarily by moving the sensors

further toward the back of the neck). It is felt that the array approach can also be very useful from the standpoint of detecting and possibly localizing blunt or penetrating trauma. By using time-difference-of-arrival information at the four acoustic sensors, a vector (magnitude and direction) can point to the site of insult and approximate the extent of damage to limb or torso. Walter Reed Army Institute of Research is currently investigating acoustic and seismic aspects of trauma and pneumothorax detection [Bentley, et. al.].

## 5. CONCLUSIONS AND FUTURE WORK:

To extract useful physiology during activity, more work needs to be conducted to reduce the effects of motion induced artifacts. From the soldier performance monitoring point of view, it may not be absolutely necessary to discern every heartbeat or breath. If the heart and breath sounds are obscured during walking or strenuous exercise, the acoustic sensor still indicates high levels of activity as shown in figure 24's stair climbing cycles. The indication of activity shows that the soldier is mobile and most likely healthy. In a tactical mission, a soldier's heart and breath sounds are significantly more detectable during low-level activity periods, and the acoustic physiology is most prominent when the soldier is either resting, lying on the ground in an unconscious state, or conscious and quietly waiting for medical attention.

ARL's Acoustic Physiological Monitoring program will continue to address the signal processing issues associated with reducing noise to enhance the physiology. The auto- and cross-correlation techniques described in this report show great promise for noise reduction. Frequency and phase spectra will also be compared to focus on the physiology. The noise-canceling array shown in figure 23 will be evaluated further, and adaptive filtering will be applied using the noise reference sensors to help minimize the noise artifacts on the physiological sensors. The sensor fusion of the acoustic and accelerometer data will be evaluated. Further investigations on the pulse wave transport time measurement for blood pressure will be conducted under controlled conditions, using a programmable blood pressure cuff for truth data. Similarly, both the noise-canceling array and the wrist/neck pulse wave transport configuration will be evaluated on subjects in more tactically significant environments. It is ARL's goal to have a single sensor on the neck that solves both the voice and physiological monitoring requirements of the Warfighter Physiological Status Monitor and the Land Warrior programs.

## REFERENCES

- Bass, James D, Scanlon, Michael V., Morgan, John J, "Getting Two Birds with One Phone: An Acoustic Sensor for Both Speech Recognition and Medical Monitoring", 138<sup>th</sup> Meeting of the Acoustical Society of America, Columbus, Ohio, 2 November 1999.
- Bentley, T., Allgood, G., Lee, J., Pierce, F., "Development of an Acoustic Method for Field Detection of Pneumothorax", Proceedings, SPIE AeroSense Battlefield Biomedical Technologies III, April 16, 2001, Vol. 4368.
- Dauzat, M., Deklunder, G., Adam, B., de Cesare, A., Ayoub, J., Masse-Biron, J., Prefaut, C. Peronneau, P., "Pulse Wave Velocity Measurement by Cross-Correlation of Doppler Velocity Signals. Application to Elderly Volunteers During Training", Int. J. Sports Med., 1996, Nov.; 17(8): 547-53,
- Kramm, S. S., "The Relationship Between Airflow and Lung Sound Amplitude in Normal Subjects", Chest, 1994; 86: pg. 225.
- Mulder, G. and L. J. M. Mulder, "Information Processing and Cardiovascular Control", Psychophysiology, 1981, 18: pp. 392-405.
- Scanlon, Michael V., "Acoustic Sensor for Health Status Monitoring", Proceedings, IRIS Acoustic and Seismic Sensing, 1998, Volume II, pp. 205-222.

*This paper was presented on April 16<sup>th</sup>, 2001 at the SPIE AeroSense2001 Conference's Battlefield Biomedical Technologies III Session (paper number 4368B-17) in Orlando, Florida, and will be published in the proceedings.*